

Bacilli Detection System in Tuberculosis Extra Pulmonary using Image Segmentation

Bob Subhan Riza¹, Jufriadif Naam², Sumijan³

¹Universitas Potensi Utama, Medan, Indonesia

^{2,3}Universitas Putra Indonesia YPTK, Padang, Indonesia

Article Info

Article history:

Received March 04, 2022

Revised August 22, 2022

Accepted October 03, 2022

Keywords:

Bacilli Detection

Image Segmentation

Tuberculosis Extra Pulmonary

ABSTRACT

Tuberculosis Extra Pulmonary (TBEP) is one of the infectious diseases that can cause death. The bacterium *Mycobacterium tuberculosis* is the cause of this disease. Patients suffering from this disease must be treated quickly. Currently, patients need a long time and a large cost in detecting the bacteria that cause this disease. The technique used is to take the patient's lung fluid by biopsy and given Ziehl Neelsen chemical dye and then observed using a microscope. This study aims to help detect bacteria quickly and precisely by processing the image produced by the microscope. The technique used is to develop the segmentation method. The segmentation process carried out is to develop a Hue Saturation Value (HSV) color space transformation technique with Active Contour, Edge Detection, and Otsu techniques. The images used in this research are 51 images taken from H. Adam Malik Hospital, Medan and have been validated by an expert. Of the several segmentation methods used in this study, the maximum or best result in detecting Tuberculosis Extra Pulmonary (TBEP) bacilli is the Otsu method. So the method developed is very helpful in accelerating the detection of TBEP.

Copyright ©2022 MATRIK: Jurnal Manajemen, Teknik Informatika, dan Rekayasa Komputer.
This is an open access article under the [CC BY-SA](#) license.



Corresponding Author:

Bob Subhan Riza,
Information System,
Universitas Potensi Utama, Medan, Indonesia,
Email: bob.potensi@gmail.com

How to Cite: B. Riza, Tuberculosis Extra Pulmonary Bacilli Detection System Based on Ziehl Neelsen Images with Segmentation, MATRIK : Jurnal Manajemen, Teknik Informatika dan Rekayasa Komputer, vol. 22, no. 1, pp. 139-148, Nov. 2022.
This is an open access article under the CC BY-NC-SA license (<https://creativecommons.org/licenses/by-nc-sa/4.0/>)

1. INTRODUCTION

Tuberculosis (TB) is a chronic and infectious disease that affects the world's human population and requires complex treatment [1], Tuberculosis, with an estimated 10 million cases and 1.3 million deaths annually, continues to be a global health priority [2], The severe acute respiratory syndrome coronavirus 2 (SARS-CoV-2) disease pandemic 2019 (COVID-19) requires concerted public health focus and action due to its rapid global spread, clinical severity, high mortality rate with 4 million deaths, and capacity for the health care system. The impact of COVID-19 on TB services has been explained by the reduction in the number of TB cases diagnosed and managed in most countries. Conservative models suggest that a 20% increase in TB deaths in the next 5 years is likely as a result of the pandemic [3]. Tuberculosis (TB) is a life-threatening infectious disease worldwide caused by the bacterium *Mycobacterium tuberculosis*. These bacteria are in the form of acid-fast bacilli or often called acid-fast bacilli (BTA). These bacilli are 1-4 μ m long and 0.3-0.56 μ m wide, non-sporing, non-motile, and facultative. Bacterial cell walls contain long-chain mycolic glycolipids, rich in acids and phosphoglycans [4-6]. Tuberculosis can attack every human being. Those of productive age are susceptible to tuberculosis between the ages of 15 and 50 years and children. Tuberculosis bacteria usually come out through phlegm and cough, if the saliva is at a low temperature, then the possibility for germs to survive will be long enough to allow the transmission process. There are 2 types of Tuberculosis, namely Pulmonary Tuberculosis (TBP) and Tuberculosis Extra Pulmonary (TBEP). TBP affects the lungs, whereas TBEP can affect any organ of the body except the spine, heart, pancreas, skeletal muscle, and thyroid [7-9]. Figure 1 below shows the *Mycobacterium Tuberculosis* bacilli.



Figure 1. *Mycobacterium Tuberculosis* [3]

The World Health Organization reports that Indonesia is the largest contributor, where Indonesia is ranked second in the world for Tuberculosis cases. In Indonesia the number increased from 331,703 in 2015 to 562,049 in 2019 (+69%) [6]. Trends in information on patients diagnosed with tuberculosis in four countries with a high TB burden can be seen in figure 2.

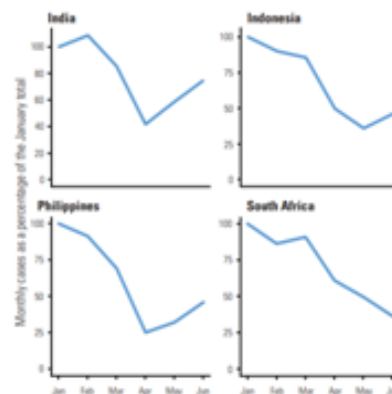


Figure 2. The trend in the monthly notification of patients diagnosed with TB in four countries with a high TB diagnosed, January-June 2020 [6]

Between January and June 2020, the number of people diagnosed with TB decreased in India, Indonesia, the Philippines, and South Africa, as the four countries that account for 44% of tuberculosis cases worldwide. Cases affected by Tuberculosis Extra Pulmonary (TBEP) accounted for 15% of 6.1 million TB cases. Tuberculosis Extra Pulmonary (TBEP) can cause complications. Based on this, a good reporting and recording system is needed for TB control [10].

Serious illness may happen to a person's lungs or other parts of the body caused by tuberculosis. Tuberculosis is spread through the air when a person with TB in the lungs coughs, sneezes, or speaks and spreads it through the air. Further spread if the germ is inhaled by a person it can be infected. Tuberculosis mostly spreads from frequent and prolonged association, for example with family members or friends. Symptoms of tuberculosis include a cough lasting more than 3 weeks, sudden weight loss, fatigue, night sweats, decreased appetite, blood-stained sputum, tuberculosis outside the lungs, pain, and swelling in the affected area. Several image processing methods have been reported for the detection of Tuberculosis Extra Pulmonary [11].

This study carried out at the stage of lung image segmentation enhanced by deep learning, disease diagnosis with artificial intelligence and aligned technology became an interesting field of research in the last decade. The novelty of this paper lies in the analysis and discussion of the results of U-Net++ and the implementation of U-Net++ on X-ray lung segmentation. Comprehensive comparison of U-Net++ with three other benchmarks of segmentation architecture and segmentation in diagnosing TB or other lung diseases, Very little segmentation is used before classification, but using only U-Net, which can be easily replaced by U-Net++ because the accuracy and mean_iou of U-Net++ is greater than the accuracy of U-Net and mean_iou, can minimize data leakage. This study resulted in lung segmentation accuracy of more than 98% and mean_iou 0.95 using U-Net ++ [12]. In other study, an attempt was made to detect the presence of bacilli in sputum smears. Smear images recorded under a standard image acquisition protocol were subjected to the Ant Colony Optimization (ACO) morphology-based segmentation procedure. This method is able to maintain the shape of the bacillus on the TB image. Shape-based features such as area, perimeter, compactness, form factor, and tortuosity are extracted from segmented images. This method retains more edges, detects the presence of bacilli and facilitates direct segmentation by reducing the number of redundant searches to generate edges [13]. Next study presents a new automated system for early detection of pulmonary TB. Initially, the Chan-Vese active contour model was created to segment lung regions from pre-processed chest radiographs. Different textural, statistical and morphological features were extracted from the segmented lungs. Finally, the feature vectors were concerned for chest X-ray classification using the Naive Bayes classifier (NBC). NBC was trained using the 10 fold cross validation technique. The proposed method achieved mean accuracy, area under the curve, specificity, and sensitivity of 95.5%, 98%, 93.3%, and 94.6%, respectively, when tested on different data sets [14]. The system automatically uses RetinaNet for segmentation of pulmonary tuberculosis bacilli. The sputum bacilloscopy method is a technique for detecting bacilli which is currently the most widely used, not only in the search for cases of infection but also as a thermometer to check the effectiveness of treatment. In this context, computational techniques have been developed to assist specialists in better diagnosis. In this study, we promote a methodology for automatic detection of bacilli using RetinaNet. A set of 928 images was used to evaluate this method. The results achieved 67.1% accuracy, 86.56% recall, and 75.61% F-score. Finally, we believe that our method is capable of acting in the diagnosis of Tuberculosis [15]. Tuberculosis detection uses chest x-ray images with deep learning, segmentation, and visualization. this study has reliably detected TB from chest X-ray images using image pre-processing, data augmentation, image segmentation, and Deep Learning classification techniques. Several public databases were used to create a database of 3500 TB infected and 3500 normal chest X-ray images. Nine CNNs were used (ResNet18, ResNet50, ResNet101, ChexNet, InceptionV3, Vgg19, DenseNet201, SqueezeNet, and MobileNet) to transfer learning from pre-trained initial weights and trained, validated, and tested to classify TB and non-TB common cases. Three different experiments were carried out in this work: segmentation of X-ray images using two different U-net models, classification using X-ray images and one using segmented lung images. The accuracy, precision, sensitivity, F1-score and specificity of the best performance model, ChexNet in tuberculosis detection using X-ray images were 96.47%, 96.62%, 96.47%, 96.47%, and 96, respectively 51%. However, classification using segmented lung images outperformed those with intact X-ray images; The accuracy, precision, sensitivity, F1-score and specificity of DenseNet201 were 98.6%, 98.57%, 98.56%, 98.56%, and 98.54% for segmented lung images, respectively. This paper also uses a visualization technique to confirm that CNN learns predominantly from segmented lung regions resulting in higher detection accuracy [16]. Research on lung image segmentation based on U-Net Deep Residual for Lung Disease Detection. This research is focused on developing a model that will segment the lungs from CXR images. By using semantic segmentation based on Residual U-Net (ResUnet) architecture, researchers can develop and train a model using 562 CXR images and lung mask images, 70% of the images are used as training data and 30% as test data. data. The model was trained with 40 epochs and a batch size of 16. Dice coefficients were used to assess the similarity of segmented results and ground truth masks. The developed model has achieved a dice coefficient of 0.9860. The developed model can then be used in classifying lung diseases [17].

2. RESEARCH METHOD

In the process of making a system to diagnose Tuberculosis Extra Pulmonary (TBEP) for the segmentation stage, several processes are carried out and can be seen in figure 3.

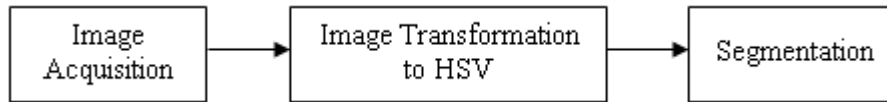


Figure 3. Block Diagram Segmentation

2.1. Image Acquisition

At the stage of taking images of Tuberculosis (TBEP) by taking fluid from a person through a biopsy, then the fluid is placed into a preparation and given Ziehl Neelsen chemical dye, so that the object to be viewed through a microscope can be seen clearly, the microscope used to take the image or disease images are already connected to a computer through an application to facilitate capture / retrieval of images from TBEP. The equipment used to analyze the slides was an Olympus BX53 digital microscope with a 10x eyepiece and a 100x objective lens for a 1000x magnification.

2.2. Image Transformation to HSV

HSV (Hue Saturation Value) color is a color that is derived from the RGB (Red Green Blue) color model, so to produce HSV colors you must go through the process of converting colors from RGB to HSV.

$$eh = \begin{cases} 0, & \text{if } \max = \min \\ 60^\circ x \left(\frac{G - B}{\max - \min} + 0 \right), & \text{if } \max = R \text{ and } G \geq B \\ 60^\circ x \left(\frac{G - B}{\max - \min} + 360 \right), & \text{if } \max = R \text{ and } G < B \\ 60^\circ x \left(\frac{B - R}{\max - \min} + 120 \right), & \text{if } \max = G \\ 60^\circ x \left(\frac{R - G}{\max - \min} + 240 \right), & \text{if } \max = B \end{cases} \quad (1)$$

$$S = \begin{cases} 0, & \text{if } \max = 0 \\ 1 - \frac{\min}{\max}, & \text{otherwise} \end{cases} \quad (2)$$

$$V = \max \quad (3)$$

where the coordinates R (Red), G (Green), B (Blue) [0,1] are sequentially red, green and blue in the RGB color space, where max is the maximum value of the red, green, blue, and min values. minimum of red, green, blue values. In the above equation, it produces value and saturation in the RGB range [0,1] by first multiplying by 255 to get a value in the RGB range [0,255].

2.3. Segmentation

In this study, the purpose of the segmentation process is to divide the network image into two regions, TBEP and non-TBEP regions. The TBEP region refers to objects that characterize TBEP bacilli while the non TBEP region refers to the background and objects in the image. In the research conducted using the Otsu thresholding algorithm for the segmentation process. The Otsu thresholding equation can be seen in equation 4.

$$\begin{aligned}\sigma^2 &= P_{nw}(M_{nw} - M)^2 + P_w(M_w - M)^2 \\ M &= P_{nw} \cdot M_{nw} + P_w \cdot M_w \\ P_{nw} + P_w &= 1\end{aligned}\quad (4)$$

$$t^* = \text{ARG Max}_{a \leq t \leq b} P_{nw}(M_{nw} - M)^2 + P_w \cdot (M_w - M)^2$$

- Where :
- σ^2 : Variants within the Tuberculosis and Non-Tuberculosis classes
 - P_{nw} : pixel value probability for non-Tuberculosis class
 - P_w : pixel value probability for Tuberculosis class
 - M_{nw} : average non-Tuberculosis class pixel value
 - M_w : Tuberculosis class average pixel value
 - M : average pixel value of the image
 - t^* : threshold value

3. RESULT AND ANALYSIS

3.1. Image Acutition

At the stage of taking images of Tuberculosis (TB) disease, namely by taking fluid from patients with Tuberculosis Extra Pulmonary through a biopsy, then the fluid is placed into preparation and given a Ziehl Neelsen chemical dye. So that the object to be viewed through a microscope can be seen clearly, the microscope used to take the image or disease pictures are already connected to a computer through an application to facilitate capture / taking pictures of Tuberculosis. The equipment used to analyze the slides was an Olympus BX53 digital microscope with a 10x eyepiece and a 100x objective lens for a 1000x magnification. The captured images are 78 images consisting of 51 TB images and 27 Non-TB images with dimensions of 1920x1440 pixels. The image or picture was taken from H. Adam Malik Central General Hospital, Medan. Tuberculosis Extra Pulmonary (TBEP) images seen under a microscope can be seen in Figure 4.

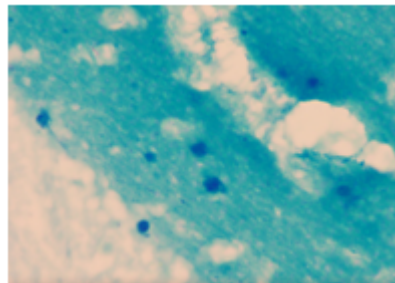


Figure 4. Image Tuberculosis Extra Pulmonary (TBEP)
(Source : RSU Pusat H. Adam Malik, 2020)

3.2. HSV Color Space Transformation

Since Hue Saturation Value (HSV) colors are derived from the Red, Green, Blue (RGB) color model, an RGB to HSV color conversion process is required to obtain an HSV color. The transformation of the RGB color space into HSV can be assumed that the coordinates R, G, B (0 or 1) are a sequence of red, green, blue in the RGB color space, max is the maximum value of the values (red, green, blue), min is the minimum value of value (red, green, blue). To get the right Hue angle [0,360] for the HSV color space, see equation 1-3 [18].

After taking Tuberculosis and Non-Tuberculosis images, the next step is to transform the HSV (Hue, Saturation, Value) color space. Hue is the actual color, Saturation is the purity of the color and Value is the brightness of the color. The advantage of using the HSV color space is that there are colors that match what is perceived by the human senses. The HSV transformed image will be used for the segmentation stage, the following is the equation for the HSV color :

The results of the HSV color can be seen in figure 5.

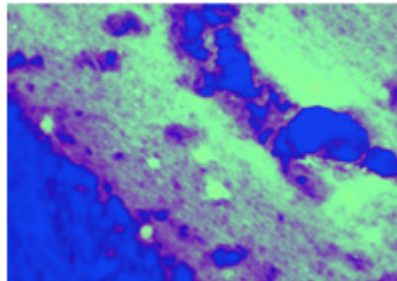


Figure 5. Image converted from RGB to HSV

The RGB image is shown in Figure 5, which is then converted to HSV (b). Converting the RGB color space to HSV, where the R, G, B coordinates (0 or 1) are the red, green, and blue color sequence in the RGB color space, where max is the maximum value of the value (red, green, blue), and min is the value of the red, green, blue color sequence. After converting the color space to HSV, the Hue component is used, because of the three HSV components that can visually distinguish between objects and the background, the Hue component is the Hue component, where the Hue component is obtained from the HSV image. The image of the Hue component can be seen in figure 6.

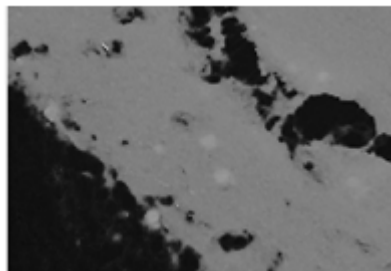


Figure 6. The result of the HSV Color Space Transformation is the Hue Component

Figure 6 shows the result of converting the HSV color space, that is, the color component, and distinguishes the object from the background.

3.3. Segmentation

Image segmentation is the identification and selection of images into specific areas to fit their structural units. Segmentation is an important operation in biomedical image processing because it is used to separate physiological and biological structures. The general approach to segmentation can be grouped into three classes: pixels, regions, and edges. In this study, the purpose of the segmentation process is to divide the network image into two regions, TB and non-TB regions. The TB region refers to objects that characterize TB bacilli while the non-TB region refers to the background and objects in the image. The research was conducted using several algorithms for the segmentation process.

Segmentation begins with reading the resulting image from the Hue component transformation, followed by calling the image resulting from the Hue component transformation. Then calculate the TBEP and non-TBEP class variants and the threshold value. When finished, the object will be separated from the background, and the Otsu thresholding image can be displayed. Then saved the image resulting from the Otsu thresholding process.

This stage performs useful segmentation to separate the required object from the background. In this segmentation process, the object of acid-fast bacilli (BTA) can be separated from other objects such as debris, cell necrosis. At this stage, it begins with calling image data from the Hue component and is processed using several segmentation methods including active contour, edge detection, and Otsu thresholding.

The following is an image of the results of several segmentation methods that have been carried out to distinguish between background and foreground :

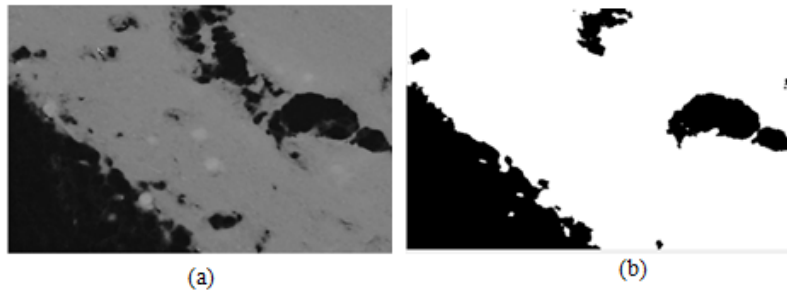


Figure 7. Segmentation results (a) Image from HSV staining technique, (b) Image from Active Contour

Figure 7 (a) segmentation results using the HSV staining technique. Figure 7 (b) is the result of using Active Contour. Segmentations result using the Active Contour method cannot show Tuberculosis Extra Pulmonary bacilli in the image used.

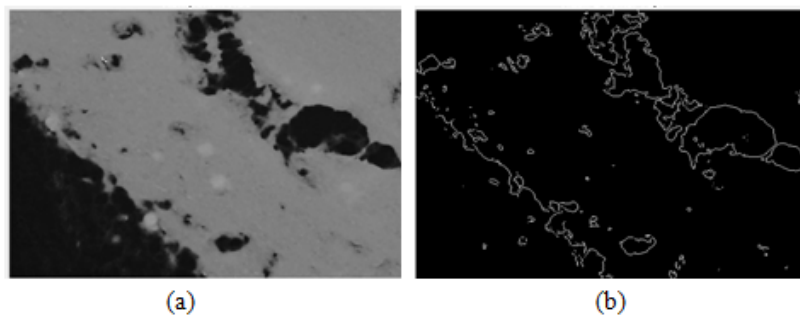


Figure 8. Segmentation results (a) Image from HSV staining technique, (b) Image from Edge Detection

Figure 8 (a) segmentation results using the HSV staining technique. Figure 8 (b) is the result using Edge Detection. Segmentation results using the Edge Detection method cannot indicate the detection of Extra Pulmonary Tuberculosis in the images used.

Otsu thresholding is used because it can produce an optimum threshold so that it can distinguish between Tuberculosis and non-Tuberculosis objects as foreground and background, The results of segmentation using otsu thresholding with HSV (Hue, Saturation, Value) staining techniques can be seen in figure 9.

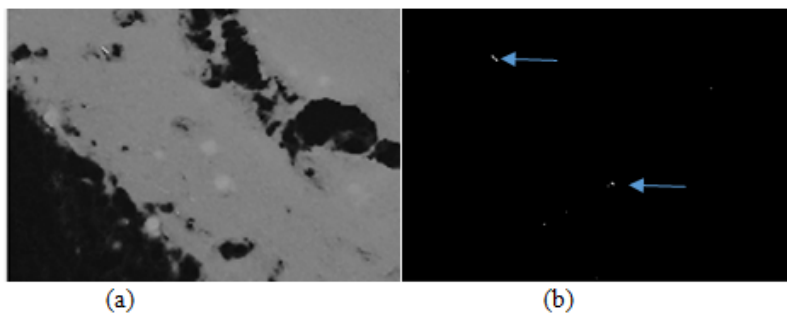


Figure 9. Segmentation results (a) Image resulting from HSV staining technique, (b) Image resulting from Otsu thresholding

Figure 9 (a) shows the segmentation result using the HSV staining technique. Figure 9 (b) is the result of thresholding using Otsu thresholding. The advantage of using Otsu thresholding is that it can calculate the threshold value automatically and maximize the variance between classes from classes separated by a threshold, which aims to separate BTA objects from the background, and accuracy is 78,68%.

This study simplifies the Mycobacterium Tuberculosis segmentation algorithm on auto-Thresholding-based sputum images. In medical image analysis, the priority is at the image segmentation stage which is still an important task today. One of the applications is to count the number of bacteria from the image of acid-fast bacilli smear preparations. A serious problem of segmentation algorithms studied in sputum culture is the problem of determining the number of bacteria. This study provides an automatic algorithm for the detection of Mycobacterium tuberculosis from AFB images, using the auto-thresholding segmentation method.

4. CONCLUSION

From the results of image retrieval that has been carried out as many as 51 images, a color transformation process will be carried out from RGB to HSV, from the results of the color transformation testing process that the Hue component. The results of the image from the Hue component can be seen from Tuberculosis Extra Pulmonary (TBEP) with different bacilli and background colors. Otsu method whose results can detect the Tuberculosis Extra Pulmonary (TBEP) bacilli clearly on the image used in this study. Next study can be color transformation with S and V component and L^*a^*b color.

5. ACKNOWLEDGEMENTS

The Acknowledgments section is optional. Research sources can be included in this section.

6. DECLARATIONS

AUTHOR CONTRIBUTION

FUNDING STATEMENT

COMPETING INTEREST

REFERENCES

- [1] F. J. Dos Santos Reist, M. A. Veloso, F. M. Moraes Rodrigues, V. De Carvalho Brito, P. R. Sales Dos Santos, J. D. L. Araujo, R. De Andrade Lira Rabelo, and A. O. De Carvalho Filho, "BacillusNet: An automated approach using RetinaNet for segmentation of pulmonary Tuberculosis bacillus," in *Proceedings - IEEE Symposium on Computers and Communications*, vol. 2021-Septe, 2021, pp. 8–11.
- [2] T. Ferkol and D. Schraufnagel, "The global burden of respiratory disease," *Annals of the American Thoracic Society*, vol. 11, no. 3, pp. 404–406, 2014.
- [3] J. Garcia and R. South-Bodiford, "Hematology," in *Small Animal Internal Medicine for Veterinary Technicians and Nurses*, J. Garcia and R. South-Bodiford, Eds. Chichester, UK: John Wiley & Sons, Ltd, oct 2017, pp. 161–192. [Online]. Available: <https://onlinelibrary.wiley.com/doi/10.1002/9781119421542.ch7>
- [4] P. Geetha Pavani, B. Biswal, M. V. Sairam, and N. Bala Subrahmanyam, "A semantic contour based segmentation of lungs from chest x-rays for the classification of tuberculosis using Naïve Bayes classifier," *International Journal of Imaging Systems and Technology*, vol. 31, no. 4, pp. 2189–2203, 2021.
- [5] ———, "A semantic contour based segmentation of lungs from chest x-rays for the classification of tuberculosis using Naïve Bayes classifier," *International Journal of Imaging Systems and Technology*, vol. 31, no. 4, pp. 2189–2203, dec 2021.
- [6] S. Gite, A. Mishra, and K. Kotecha, "Enhanced lung image segmentation using deep learning," *Neural Computing and Applications*, vol. 8, no. January, pp. 1–15, jan 2022. [Online]. Available: <https://doi.org/10.1007/s00521-021-06719-8https://link.springer.com/10.1007/s00521-021-06719-8>

- [7] H. Hartatik, "Diagnosa Penyakit Pulmonary Tuberculosis Dan Extrapulmonary Tuberculosis Menggunakan Algoritma Certainty Factor (CF)," *CSRID (Computer Science Research and Its Development Journal)*, vol. 8, no. 1, pp. 11–24, mar 2016.
- [8] I. Kurniastuti, T. D. Wulan, and A. Andini, "Color Feature Extraction of Fingernail Image based on HSV Color Space as Early Detection Risk of Diabetes Mellitus," in *2021 International Conference on Computer Science, Information Technology, and Electrical Engineering (ICOMITEE)*, no. October. IEEE, oct 2021, pp. 51–55. [Online]. Available: <https://ieeexplore.ieee.org/document/9650161/>
- [9] G. B. Migliori, N. Casco, A. L. Jorge, D. J. Palmero, J. W. Alffenaar, J. Denholm, G. J. Fox, W. Ezz, J. G. Cho, A. Skrahina, V. Solodovnikova, P. Bachez, A. Piubello, M. A. Arbex, T. Alves, M. F. Rabahi, G. R. Pereira, R. Sales, D. R. Silva, M. M. Saffie, R. C. Miranda, V. Cancino, M. Carbonell, C. Cisterna, C. Concha, A. Cruz, N. E. Salinas, M. E. Revillot, J. F. Valdés, I. Fernandez, X. Flores, P. G. Tapia, A. Garavagno, C. G. Vera, M. H. Bahamondes, L. M. Merino, E. Muñoz, C. Muñoz, I. Navarro, J. N. Subiabre, C. Ortega, S. Palma, A. M. Pradenas, G. Pereira, P. P. Castillo, M. Pinto, R. Pizarro, F. R. Bidegain, P. Rodriguez, C. Sánchez, A. S. Salinas, A. Soto, C. Taiba, M. Venegas, M. S. V. Riquelme, E. Vilca, C. Villalón, E. Yucra, Y. Li, A. Cruz, B. Guelvez, R. V. Plaza, K. Y. T. Hoyos, C. Andr jak, F. X. Blanc, S. Dourmane, A. Froissart, A. Izadifar, F. Riviere, F. Schlemmer, K. Manika, B. D. Diallo, S. Hassane-Harouna, N. Artiles, L. A. Mejia, N. Gupta, P. Ish, G. Mishra, S. Sharma, R. Singla, Z. F. Udwadia, F. Alladio, F. Angeli, A. Calcagno, R. Centis, L. R. Codecasa, L. D'Ambrosio, A. De Lauretis, S. Esposito, B. Formenti, A. Gaviraghi, V. Giacomet, D. Goletti, G. Gualano, A. Matteelli, G. B. Migliori, I. Motta, F. Palmieri, E. Pontali, T. Prestileo, N. Riccardi, L. Saderi, M. Saporiti, G. Sotgiu, C. Stochino, M. Tadolini, A. Torre, S. Villa, D. Visca, E. Danila, S. Diktanas, R. L. Ridaura, F. L. L. L pez, M. M. Torrico, A. Rendon, O. W. Akkerman, M. B. Souleymane, S. Al-Abri, F. Alyaquobi, K. Althohli, E. Aizpurua, R. Gonzales, J. Jurado, A. Loban, S. Aguirre, R. C. Teixeira, V. De Egea, S. Irala, A. Medina, G. Sequera, N. Sosa, F. V zquez, F. K. Llanos-Tejada, S. Manga, R. Villanueva-Villegas, D. Araujo, R. Duarte, T. S. Marques, V. I. Grecu, A. Socaci, O. Barkanova, M. Bogorodskaya, S. Borisov, A. Mariandyshev, A. Kaluzhenina, T. A. Vukicevic, M. Stosic, D. Beh, D. Ng, C. W. Ong, I. Solovic, K. Dheda, P. Gina, J. A. Caminero, J. Cardoso-Landivar, M. L. De Souza Galv o, A. Dominguez-Castellano, J. M. Garc a-Garc a, I. M. Pinargote, S. Q. Fernandez, A. S nchez-Montalv a, E. T. Huguet, M. Z. Murguiondo, P. A. Bart, J. Mazza-Stalder, F. Bakko, J. Barnacle, A. Brown, S. Chandran, K. Killington, K. Man, P. Papineni, S. Tiberi, N. Utjesanovic, D. Zenner, J. L. Hearn, S. Heysell, and L. Young, "Tuberculosis and COVID-19 co-infection: description of the global cohort," *European Respiratory Journal*, vol. 59, no. 3, pp. 1–15, 2022. [Online]. Available: <http://dx.doi.org/10.1183/13993003.02538-2021>
- [10] E. Mique and A. Malicdem, "Deep Residual U-Net Based Lung Image Segmentation for Lung Disease Detection," in *IOP Conference Series: Materials Science and Engineering*, vol. 803, no. 1, apr 2020, pp. 1–8. [Online]. Available: <https://iopscience.iop.org/article/10.1088/1757-899X/803/1/012004>
- [11] A. Rachmad, N. Chamidah, and R. Rulaningtyas, "Mycobacterium tuberculosis identification based on colour feature extraction using expert system," *Annals of Biology*, vol. 36, no. 2, pp. 196–202, 2020.
- [12] T. Rahman, A. Khandakar, M. A. Kadir, K. R. Islam, K. F. Islam, R. Mazhar, T. Hamid, M. T. Islam, S. Kashem, Z. B. Mahbub, M. A. Ayari, and M. E. Chowdhury, "Reliable tuberculosis detection using chest X-ray with deep learning, segmentation and visualization," in *IEEE Access*, vol. 8, 2020, pp. 191 586–191 601.
- [13] B. S. Riza, M. Y. Mashor, M. K. Osman, and H. Jaafar, "Automated segmentation procedure for Ziehl-Neelsen stained tissue slide images," in *2017 5th International Conference on Cyber and IT Service Management (CITSM)*. IEEE, aug 2017, pp. 1–5. [Online]. Available: <http://ieeexplore.ieee.org/document/8089292/>
- [14] —, "Segmentation for Tuberculosis Ziehl-Neelsen Stained Tissue Slide Image Using Thresholding," in *2018 6th International Conference on Cyber and IT Service Management, CITSM 2018*, vol. Agustus. IEEE, 2019, pp. 8–10.
- [15] D. R. Silva, A. A. Freitas, A. R. Guimar es, L. D'ambrosio, R. Centis, M. Mu oz-Torrico, D. Visca, and G. B. Migliori, "Post-tuberculosis lung disease: a comparison of Brazilian, Italian, and Mexican cohorts," *Jornal Brasileiro de Pneumologia*, vol. 48, no. 2, pp. 6–11, 2022.
- [16] F. F. Suharto, E. N. Fetriawan, M. S. Y. Pratama, R. D. Ananda, Z. Ahmad, R. A. L. Andrian, and H. Hudari, "Jurnal RSMH Palembang," *Jurnal RSMH Palembang*, vol. 1, no. 1, pp. 31–40, 2020.

- [17] R. Ullah, S. Khan, Z. Ali, H. Ali, A. Ahmad, and I. Ahmed, "Evaluating the performance of multilayer perceptron algorithm for tuberculosis disease Raman data," *Photodiagnosis and Photodynamic Therapy*, vol. 39, no. January, p. 102924, 2022. [Online]. Available: <https://doi.org/10.1016/j.pdpdt.2022.102924>
- [18] S. A. Wulandari, D. A. Mayasari, M. D. Kurniatie, and R. Tjahyono, "Simplification of Mycobacterium Tuberculosis Segmenting Algorithm in Sputum Images Based of Auto-Thresholding," in *2021 International Seminar on Application for Technology of Information and Communication (iSemantic)*. IEEE, sep 2021, pp. 12–16. [Online]. Available: <https://ieeexplore.ieee.org/document/9573219/>